JACS
JOURNAL OF THE AMERICAN CHEMICAL SOCIETY

COMMUNICATION

pubs.acs.org/JACS

Hydrogen Bonding of Tryptophan Radicals Revealed by EPR at 700 GHz

Stefan Stoll,*[,†,∥] Hannah S. Shafaat,[‡] J. Krzystek,[§] Andrew Ozarowski,[§] Michael J. Tauber,[‡] Judy E. Kim,[‡] and R. David Britt*[,†]

[†]Department of Chemistry, University of California Davis, Davis, California 95616, United States

[‡]Department of Chemistry and Biochemistry, University of California San Diego, La Jolla, California 92093, United States

[§]National High Magnetic Field Laboratory, Florida State University, Tallahassee, Florida 32310, United States

Supporting Information

ABSTRACT: Redox-active tryptophans are important in biological electron transfer and redox biochemistry. Proteins can tune the electron transfer kinetics and redox potentials of tryptophan via control of the protonation state and the hydrogen-bond strength. We examine the local environment of two neutral tryptophan radicals (Trp108 on the solvent-exposed surface and Trp48 buried in the hydrophobic core) in two azurin variants. Ultrahigh-field EPR spectroscopy at 700 GHz and 25 T allowed complete resolution of all of the principal components of the **g** tensors of the two radicals and revealed significant differences in the **g** tensor anisotropies. The spectra together with ^{2}H ENDOR spectra and supporting DFT calculations show that the **g** tensor anisotropy is directly diagnostic of the presence or absence as well as the strength of a hydrogen bond to the indole nitrogen. The approach is a powerful one for identifying and characterizing hydrogen bonds that are critical in the regulation of tryptophan-assisted electron transfer and tryptophan-mediated redox chemistry in proteins.

Redox-active tryptophans play important roles in proteins. They serve as relays in long-range electron transfer, e.g., in photolyases[1] and cryptochromes[2] as well as in engineered proteins.[3−5] In cytochrome *c* peroxidase and related enzymes, oxidized tryptophans located near the heme active sites provide a strong oxidation equivalent.[6,7] In some peroxidases with lignolytic activity,[8] surface-exposed tryptophans are the active high-potential oxidants that enable degradation of the recalcitrant substrate lignin. This functionality can be engineered into other peroxidases[9] by incorporating the tryptophan and its binding pocket.

The pH-dependent redox potential of tryptophan (TrpH) is ∼1.0 V at pH 7, ∼0.1 V above that of tyrosine.[10] Upon oxidation of TrpH, the pK_a of the hydrogen at the indole nitrogen N1 drops from ∼17 in TrpH to ∼4 in the cation radical $Trp^{\bullet}H^{+}$. As a consequence, oxidation in nonacidic environments is accompanied or followed by deprotonation,[11] resulting in the neutral radical $Trp^{\bullet}$. Proteins can adjust the reactivity of the Trp radical by controlling this deprotonation. Finer control over the thermodynamic and kinetic behavior of TrpH oxidation, which is especially important in electron transfer, can be accomplished by providing hydrogen-bonding partners to N1 and varying the strength of the available H-bonds.

Unlike in tyrosyl radicals,[4,12−16] hydrogen bonds are difficult to observe directly in oxidized Trp,[17,18] and consequently, little is known about their impact on Trp reactivity. Here we show that the H-bond environment can be directly identified via the magnetic structure of the Trp radicals. We have found that the anisotropy of the **g** tensors of the Trp radicals, which can be resolved using ultrahigh-field electron paramagnetic resonance (EPR) spectroscopy, reveals the presence or absence as well as the strength of an H-bond to the indole nitrogen.

For this study, model tryptophan radicals photogenerated in two different variants of the copper protein azurin were used.[18] In a tyrosine-depleted azurin mutant (AzC), direct photoexcitation of the native Trp48 in the hydrophobic core of the protein induces intraprotein electron transfer over 10 Å to Cu(II) combined with deprotonation of the indole nitrogen, resulting in a neutral $Trp^{\bullet}$ radical.[18] In another modified azurin (ReAzS), the surface-exposed non-native Trp108 is situated in a hydrophilic environment and can be oxidized via a Re(I) phototrigger attached to His107.[18,19] After deprotonation, a neutral $Trp^{\bullet}$ radical is generated. The two radicals are located in different environments, which affect their spectroscopic properties.

Figure 1 shows the X-band EPR spectra of the two Trp radicals. Both saturate easily, and lower temperatures or higher microwave power levels lead to broadening [see the Supporting Information (SI)]. The spectra are rich in hyperfine structure and can be simulated as neutral $Trp^{\bullet}$ radicals. The hyperfine parameters compare well with those from a previous report[18] and those of $Trp^{\bullet}$ in RNR mutants[17,20,21] and versatile peroxidases.[22−24] The radicals are not cationic $Trp^{\bullet}H^{+}$, as observed in cytochrome *c* peroxidase[6] and in acidic aqueous solution,[25,26] since the spectra show only miniscule changes upon ^{1}H/^{2}H exchange and the ^{1}H electron−nuclear double resonance (ENDOR) spectra lack peaks due to a proton at N1 (see the SI). According to the hyperfine couplings, the spin density is mostly concentrated on C3 (∼0.5), N1 (∼0.3), C5, and C7. The difference between the two spectra is largely due to a 10° difference in the dihedral angle $\chi_{2,1}$ (Cα−Cβ−C3−C2). The spectra are slightly asymmetric as a result of an unresolved small **g** tensor anisotropy corresponding to ∼0.2 mT.

The **g** tensor anisotropy can be resolved using high-field EPR spectroscopy. For tyrosyl radicals with their larger **g** anisotropy,

Received: September 7, 2011
Published: October 18, 2011

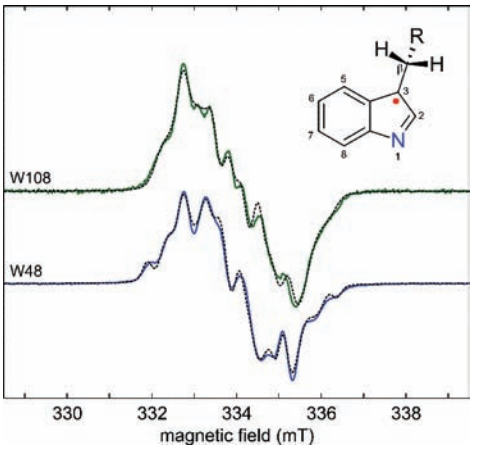

Figure 1. X-band EPR spectra of Trp radicals in azurin mutants in ^1H_2O, 20% glycerol: (top) Trp108 in ReAzS; (bottom) Trp48 in AzC. Recorded at 9.38 GHz, 200 K, 2 μW. Solid lines are experimental spectra; dashed lines are simulations (see the SI for details).

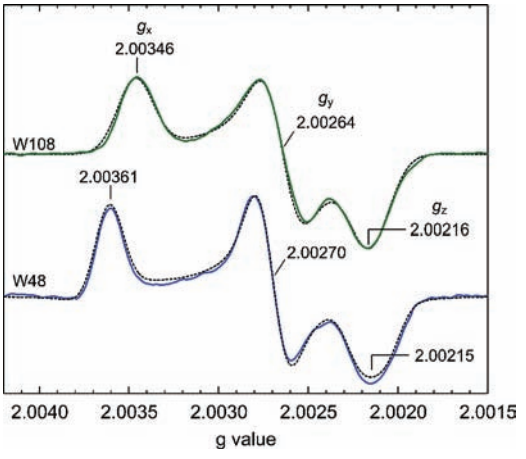

Figure 2. Ultrahigh-field EPR spectra of Trp radicals in azurin mutants in ^1H_2O, 20% glycerol: (top) Trp108 in ReAzS; (bottom) Trp48 in AzC. Recorded at 687−695 GHz, 24.8 T, 5 K. Solid lines are averages of experimental spectra; dashed lines are simulations. The absolute error for the g values is 0.00010, and the error of differences such as $g_x - g_z$ is 0.00003.

95 GHz/3.3 T is sufficient,[27] but Trp radical **g** tensors are less anisotropic and are only partially resolved even at 285 GHz/10.2 T.[9,19,28] The separation of the features corresponding to the three principal g values is complete only at ultrahigh fields and frequencies (25 T, 700 GHz),[29−31] as shown in Figure 2. The values, calibrated against an atomic H standard,[32] are (g_x, g_y, g_z) = (2.00346, 2.00264, 2.00216) for ReAzS-Trp108 and (2.00361, 2.00270, 2.00215) for AzC-Trp48. The Trp48 **g** tensor is similar to the earlier one derived from a partially resolved 285 GHz spectrum.[19] The high-resolution spectra shown in Figure 2 were measured at the highest field and frequency achieved to date for organic radicals. The hyperfine structure was lost because of magnetic field inhomogeneity.

What causes the difference in the **g** tensors? Density functional theory (DFT) indicates that the dihedral angle $\chi_{2,1}$ can affect the **g** tensor by modulating the spin density at N1 (see the SI). However, the $\chi_{2,1}$ values for the two radicals are similar, and this

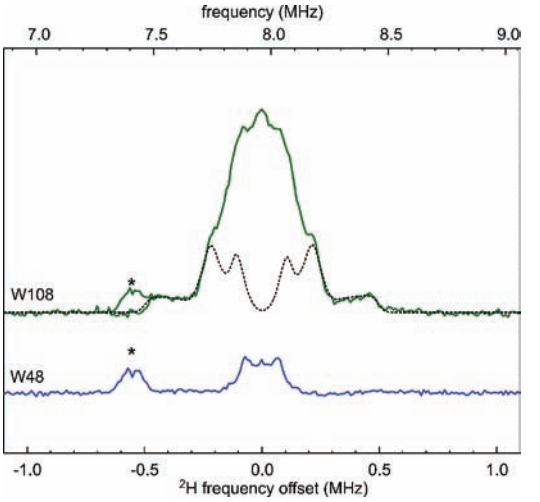

Figure 3. Q-band ^{2}H Mims ENDOR spectra of ReAzS-Trp108 and AzC-Trp48, both in ^2H_2O, recorded at 20 K and 1.218 T. Microwave pulse lengths, 36 ns; rf pulse length, 75 μs; τ = 600 ns; repetition time, 1 s. Solid lines, experimental; dashed, simulation. The zero of the frequency offset denotes the ^{2}H Larmor frequency, which is 1/6.511 of the ^{1}H Larmor frequency. The asterisks indicate the seventh harmonic of the ^{1}H spectrum.

explanation can only account for about a sixth of the observed difference $g_x - g_z$. The other major structural determinant in the microenvironment is the presence or absence of a hydrogen bond to the indole nitrogen. The crystal structure of ReAzS (PDB entry 1R1C) shows the partial presence of a water oxygen atom 2.3 Å from N1 of nonoxidized Trp108. Assuming a N−H distance of 1.0 Å implies a (N)H···O distance of 1.3 Å, indicative of a strong H-bond.[33] Whether this H-bond persists after oxidation is unknown. Its presence in the radical form (as N···HX) in solution was inferred from the frequency of the W17 mode of the radical as measured by resonance Raman spectroscopy.[18] Also, upon ^{1}H/^{2}H exchange, the X-band EPR spectrum of Trp108 sharpens slightly, and its ^{1}H ENDOR spectrum shows distinctive loss of signal around the ^{1}H Larmor frequency (see the SI), both suggesting the presence of an H-bond. However, the aforementioned facts constitute only indirect evidence for an H-bond.

Direct evidence for the H-bond to the Trp108 radical is seen in the ^{2}H ENDOR spectrum of a sample prepared in ^2H_2O (Figure 3 top), which shows a signal from a fairly strongly coupled ^{2}H. Simulation gave a ^{2}H quadrupole coupling constant e^2qQ/h = 0.16(1) MHz, which is smaller than that in ^2H_2O ice (0.2134 MHz)[34] but similar to that in ^{2}H-bonded semiquinone or tyrosyl radicals.[35−39] The coupling constant is consistent with the deuteron participating in an H-bond to N1. The asymmetry of the quadrupole tensor, η = 0.10(2), is typical for water (^2H_2O: 0.112) and suggests water as the H-bond partner. The ^{2}H hyperfine tensor with principal values ($a_{iso} - T$, $a_{iso} - T$, $a_{iso} + 2T$) is approximately axial with an isotropic component a_{iso} = 0.03(2) MHz and a dipolar component T = 0.36(3) MHz. The very small a_{iso} indicates a spin population of (0.03)(6.511)/1420 ≈ 0.1% on the hydrogen, again consistent with a noncovalent H-bond. From T and a typical spin population of ∼0.3 on the indole nitrogen, a N···H distance of ∼2 Å can be estimated.

In contrast to Trp108, the ^{2}H ENDOR spectrum of Trp48 (Figure 3 bottom) lacks features that would indicate deuterons

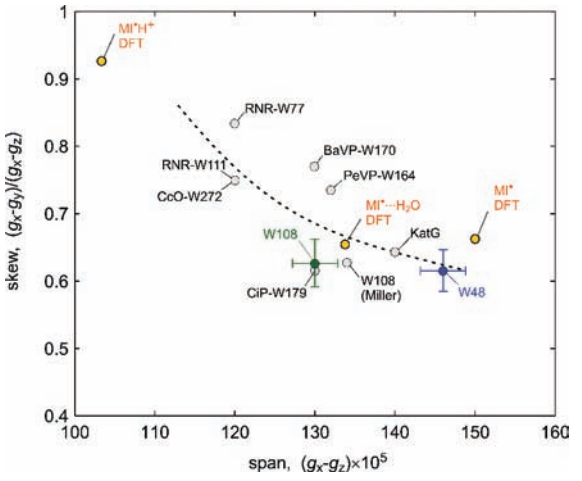

Figure 4. Comparison of known **g** tensors of Trp radicals: W48 and W108, this work; W108 (Miller), an earlier W108 value;[19] RNR-W77 and RNR-W111, ribonucleotide reductase mutants;[17] BaVP, *B. adusta* versatile peroxidase;[22] PeVP, *P. eryngii* versatile peroxidase;[23] CcO, cytochrome *c* oxidase;[40] KatG: catalase−peroxidase;[28] CiP: *C. cinereus* peroxidase mutant[9] (see the SI for a list). Values for the neutral and cation radical of 3-methylindole (MI) calculated using DFT in vacuo are included as well. The dashed line visually indicates the span/skew correlation.

close to the Trp radical. The 0.3 MHz total width of the observed ^{2}H matrix peak implies $T < 0.08$ MHz, meaning that the closest deuteron is at least 3 Å away from the indole nitrogen. Consequently, Trp48 is not H-bonded. We cannot logically eliminate the possibility that the ^{1}H released by Trp48 after oxidation remains H-bonded to N1 and does not exchange with the solvent in the time before the freeze-quench (∼1 min). However, this is unlikely since (a) there are no potential H-bond partners in the immediate vicinity of the Trp48 indole nitrogen and (b) the shifts in several Raman modes relative to Trp108 corroborate the absence of an H-bond.[18] Collectively, the ^{2}H ENDOR data show that the significant difference in the two **g** tensors correlates with the absence or presence of an H-bond.

Figure 4 compares the two measured **g** tensors to DFT-predicted **g** tensors of the isolated neutral, H-bonded neutral, and isolated cation radicals of 3-methylindole (see the SI).[41] The experimentally observed trend is reproduced: In the absence of a hydrogen bond, the **g** tensor is most anisotropic with the largest span, $g_x - g_z$, and the smallest skew, $(g_x - g_y)/(g_x - g_z)$. With an H-bond, the span shrinks substantially as a result of the decreased g_x value. DFT predicts that the span would be smallest and the skew largest in the protonated cation radical. The agreement between theory and experiment indicates that the H-bond is responsible for the decrease in **g** anisotropy in Trp108 relative to Trp48 and that other local effects on the **g** tensor (from $\chi_{2,1}$, interactions with the π spin density, etc.) are most likely insignificant. It should be noted that in contrast to ^{2}H ENDOR, the **g** tensor anisotropy can reveal the absence of an H-bond, not only its presence. Figure 4 includes the few other (less accurately) known Trp **g** tensors,[9,17,20,22,23,28,40] which have $g_x - g_z$ values between 0.0012 and 0.0014. These values are similar to the span of Trp108 and clearly smaller than that of Trp48, indicating that all of these Trp radicals are H-bonded, with possible exception of the one in KatG. Among H-bonded radicals, the variation in $g_x - g_z$ might report on the strength of the H-bond.

The trend in Figure 4 can be rationalized on the basis of a per-atom breakdown of the DFT-predicted **g** tensors.[42] On each atom, the *g* shifts $\Delta g_{x,y,z} = g_{x,y,z} - g_e$ depend on the spin population and spin−orbit coupling and originate from excitations of electrons between filled and half-filled orbitals perpendicular to the magnetic field axis.[17,27] In the isolated neutral radical, the g_x shift $\Delta g_x = g_x - g_e$ is dominated by the contribution from N1 (80%), with a small contribution (10%) from C3, the other atom with a large spin population. Upon H-bonding, the N1 contribution to Δg_x decreases, whereas the C3 contribution remains unchanged. H-bonding lowers the energy of the non-bonding MO that contains the in-plane lone-pair orbital on N1, resulting in an increased energy gap to the singly occupied molecular orbital (SOMO) and thus to a decreased *g* shift along a direction (denoted *x*) perpendicular to both the N1 lone-pair orbital and the SOMO. The computed N1 spin populations do not vary significantly with H-bonding, although the experimental N1 hyperfine couplings indicate that the N1 spin density in Trp108 is lower than that in Trp48. The value of Δg_y is less sensitive to H-bonding. It is a sum over several atomic contributions (from N1, C2, C3, C5, and C7) with similar magnitudes but different signs. Upon variation of the H-bonding, these contributions all undergo small changes that are mostly due to shifts in the spin density distribution, giving in toto only a small change in Δg_y. The deviations of g_z from g_e are negligibly small. The **g** tensor anisotropies of all Trp radicals are much smaller than those of tyrosyl radicals ($TyrO^\bullet$), which have $g_x - g_z = 0.004$ to 0.007 depending on the presence of H-bonds to the phenoxy oxygen.[16,27] This is a consequence of the smaller charge and spin−orbit coupling of the nitrogen nucleus in $Trp^\bullet$ relative to oxygen in $TyrO^\bullet$.

To summarize: (1) By employing EPR spectroscopy at ultrahigh field and frequency, we could completely resolve the very small **g** anisotropies of two model Trp radicals. The anisotropies of the two **g** tensors differ substantially. (2) ^{2}H ENDOR spectra showed the presence of a hydrogen bond to Trp108 but none to Trp48. (3) The experimental findings, in tandem with DFT calculations, established a clear correlation between the **g** tensor and the H-bond properties of Trp radicals: smaller **g** anisotropy indicates a H-bond to the indole nitrogen, whereas larger **g** anisotropy indicates the absence of a H-bond. (4) We expect this correlation to be helpful in identifying H-bonds and studying their role in the regulation of tryptophan-assisted electron transfer in proteins and tryptophan-mediated redox chemistry, which are both crucial in a variety of natural processes such as DNA repair and the biodegradation of lignin. A clear understanding of H-bonding to tryptophans is also essential for deploying them as components in engineered proteins and enzymes.

■ ASSOCIATED CONTENT

Supporting Information. Materials and methods; EPR power saturation and room-temperature spectra; EPR and ^{1}H ENDOR spectra after ^{1}H/^{2}H exchange; EPR simulation details; published Trp **g** tensors; details on DFT prediction of **g** tensors; and spin density distribution. This material is available free of charge via the Internet at http://pubs.acs.org.

■ AUTHOR INFORMATION

Corresponding Author
ststst@uw.edu; rdbritt@ucdavis.edu

Present Addresses
[||]Department of Chemistry, University of Washington, Box 351700, Seattle, WA 98195, United States.

■ ACKNOWLEDGMENT

This work was supported by NSF (CHE-0911766, J.E.K.), NIH (GM-73789, R.D.B.), and DOE (DE-FG02-09ER16117, R.D.B.). A portion of this work was performed at the National High Magnetic Field Laboratory, which is funded by the NSF (DMR-0654118), the State of Florida, and the U.S. Department of Energy. H.S.S. was supported by an NSF Graduate Research Fellowship. We thank Dr. Stephen Hill for the microwave measurements and Dr. Brian Leigh for the synthesis of the Re compound.

■ REFERENCES

(1) Brettel, K.; Byrdin, M. *Curr. Opin. Struct. Biol.* **2010**, *20*, 693.
(2) Langenbacher, T.; Immeln, D.; Dick, B.; Kottke, T. *J. Am. Chem. Soc.* **2009**, *131*, 14274.
(3) Shih, C.; Museth, A. K.; Abrahamsson, M.; Blanco-Rodriguez, A. M.; Di Bilio, A. J.; Sudhamsu, J.; Crane, B. R.; Ronayne, K. L.; Towrie, M.; Vlcek, A., Jr.; Richards, J. H.; Winkler, J. R.; Gray, H. B. *Science* **2008**, *320*, 1760.
(4) Yeh, H. C.; Gerfen, G. J.; Wang, J. S.; Tsai, A. L.; Wang, L. H. *Biochemistry* **2009**, *48*, 917.
(5) Gray, H. B.; Winkler, J. R. *Biochim. Biophys. Acta* **2010**, *1797*, 1563.
(6) Huyett, J. E.; Doan, P. E.; Gurbiel, R.; Houseman, A. L. P.; Sivaraja, M.; Goddin, D. B.; Hoffman, B. M. *J. Am. Chem. Soc.* **1995**, *117*, 9033.
(7) Jasion, V. S.; Polanco, J. A.; Meharenna, Y. T.; Li, H.; Poulos, T. L. *J. Biol. Chem.* **2011**, *286*, 24608.
(8) Hammel, K. E.; Cullen, D. *Curr. Opin. Plant Biol.* **2008**, *11*, 349.
(9) Smith, A. T.; Doyle, W. A.; Dorlet, P.; Ivancich, A. *Proc. Natl. Acad. Sci. U.S.A.* **2009**, *106*, 16084.
(10) Harriman, A. *J. Phys. Chem.* **1987**, *91*, 6102.
(11) Zhang, M.-T.; Hammarström, L. *J. Am. Chem. Soc.* **2011**, *133*, 8806.
(12) Engström, M.; Himo, F.; Gräslund, A.; Minaev, B.; Vahtras, O.; Ågren, H. *J. Phys. Chem. A* **2000**, *104*, 5149.
(13) Faller, P.; Coussias, C.; Rutherford, A. W.; Un, S. *Proc. Natl. Acad. Sci. U.S.A.* **2003**, *100*, 8732.
(14) Svistunenko, D. A.; Cooper, C. E. *Biophys. J.* **2004**, *87*, 582.
(15) Matsuoka, H.; Shen, J.-R.; Kawamori, A.; Nishiyama, K.; Ohba, Y.; Yamauchi, S. *J. Am. Chem. Soc.* **2011**, *133*, 4655.
(16) Bennati, M.; Stubbe, J.; Griffin, R. G. *Appl. Magn. Reson.* **2001**, *21*, 389.
(17) Bleifuss, G.; Kolberg, M.; Pötsch, S.; Hofbauer, W.; Bittl, R.; Lubitz, W.; Gräslund, A.; Lassmann, G.; Lendzian, F. *Biochemistry* **2001**, *40*, 15362.
(18) Shafaat, H. S.; Leigh, B. S.; Tauber, M. J.; Kim, J. E. *J. Am. Chem. Soc.* **2010**, *132*, 9030.
(19) Miller, J. E.; Grădinaru, C.; Crane, B. R.; Di Bilio, A. J.; Wehbi, W. A.; Un, S.; Winkler, J. R.; Gray, H. B. *J. Am. Chem. Soc.* **2003**, *125*, 14220.
(20) Lendzian, F.; Sahlin, M.; MacMillan, F.; Bittl, R.; Fiege, R.; Pötsch, S.; Sjöberg, B.-M.; Gräslund, A.; Lubitz, W.; Lassmann, G. *J. Am. Chem. Soc.* **1996**, *118*, 8111.
(21) Pötsch, S.; Lendzian, F.; Ingemarson, R.; Hörnberg, A.; Thelander, L.; Lubitz, W.; Lassmann, G.; Gräslund, A. *J. Biol. Chem.* **1999**, *274*, 17696.
(22) Pogni, R.; Baratto, M. C.; Giansanti, S.; Teutloff, C.; Verdin, J.; Valderrama, B.; Lendzian, F.; Lubitz, W.; Vazquez-Duhalt, R.; Basosi, R. *Biochemistry* **2005**, *44*, 4267.
(23) Pogni, R.; Baratto, M. C.; Teutloff, C.; Giansanti, S.; Ruiz-Dueñas, F. J.; Choinowski, T.; Piontek, K.; Martínez, A. T.; Lendzian, F.; Basosi, R. *J. Biol. Chem.* **2006**, *281*, 9517.
(24) Pogni, R.; Teutloff, C.; Lendzian, F.; Basosi, R. *Appl. Magn. Reson.* **2007**, *31*, 509.
(25) Kiryutin, A. S.; Morozova, O. B.; Kuhn, L. T.; Yurkovskaya, A. V.; Hore, P. J. *J. Phys. Chem. B* **2007**, *111*, 11221.
(26) Connor, H. D.; Sturgeon, B. E.; Mottley, C.; Sipe, H. J., Jr.; Mason, R. P. *J. Am. Chem. Soc.* **2008**, *130*, 6381.
(27) Stoll, S. In *Electron Paramagnetic Resonance*; Gilbert, B. C., Chechik, V., Murphy, D. M., Eds.; Royal Society of Chemistry: Cambridge, U.K., 2011; Vol. 22, p 107.
(28) Colin, J.; Wiseman, B.; Switala, J.; Loewen, P. C.; Ivancich, A. *J. Am. Chem. Soc.* **2009**, *131*, 8557.
(29) Konovalova, T. A.; Krzystek, J.; Bratt, P. J.; van Tol, J.; Brunel, L.-C.; Kispert, L. D. *J. Phys. Chem. B* **1999**, *103*, 5782.
(30) Bratt, P. J.; Ringus, E.; Hassan, A. K.; van Tol, J.; Maniero, A. L.; Brunel, L.-C.; Rohrer, M.; Bubenzer-Hange, C.; Scheer, H.; Angerhofer, A. *J. Phys. Chem. B* **1999**, *103*, 10973.
(31) Bratt, P. J.; Heathcote, P.; Hassan, A.; van Tol, J.; Brunel, L.-C.; Schrier, J.; Angerhofer, A. *Chem. Phys.* **2003**, *294*, 277.
(32) Stoll, S.; Ozarowski, A.; Britt, R. D.; Angerhofer, A. *J. Magn. Reson.* **2010**, *207*, 158.
(33) Steiner, T. *Angew. Chem., Int. Ed.* **2002**, *41*, 48.
(34) Edmonds, D. T.; Mackay, A. L. *J. Magn. Reson.* **1975**, *20*, 515.
(35) van Dam, P. J.; Willems, J.-P.; Schmidt, P. P.; Pötsch, S.; Barra, A.-L.; Hagen, W. R.; Hoffman, B. M.; Andersson, K. K.; Gräslund, A. *J. Am. Chem. Soc.* **1998**, *120*, 5080.
(36) Bar, G.; Bennati, M.; Nguyen, H.-H. T.; Ge, J.; Stubbe, J.; Griffin, R. G. *J. Am. Chem. Soc.* **2001**, *123*, 3569.
(37) Flores, M.; Isaacson, R. A.; Calvo, R.; Feher, G.; Lubitz, W. *Chem. Phys.* **2003**, *294*, 401.
(38) Flores, M.; Isaacson, R.; Abresch, E.; Calvo, R.; Lubitz, W.; Feher, G. *Biophys. J.* **2007**, *92*, 671.
(39) Kessen, S.; Teutloff, C.; Kern, J.; Zouni, A.; Bittl, R. *ChemPhysChem* **2010**, *11*, 1275.
(40) Wiertz, F. G. M.; Richter, O.-M. H.; Ludwig, B.; de Vries, S. *J. Biol. Chem.* **2007**, *282*, 31580.
(41) Un, S. *Magn. Reson. Chem.* **2005**, *43*, S229.
(42) Stone, A. J. *Proc. R. Soc. London* **1963**, *271*, 424.